ARTICLE

Benzaldehyde-Functionalized Polymer Vesicles

Guorong Sun,[†] Huafeng Fang,[†] Chong Cheng,[‡] Peng Lu,[†] Ke Zhang,[†] Amy V. Walker,[†] John-Stephen A. Taylor,[†] and Karen L. Wooley[†,*]

[†]Departments of Chemistry and Radiology, and Center for Materials Innovation, Washington University in Saint Louis, Saint Louis, Missouri 63130 and [‡]Department of Chemical and Biological Engineering, State University of New York at Buffalo, Buffalo, New York 14260

ABSTRACT Polymer vesicles with diameters of *ca.* 100−600 nm and bearing benzaldehyde functionalities within the vesicular walls were constructed through self-assembly of an amphiphilic block copolymer PEO_{45}-*b*-$PVBA_{26}$ in water. The reactivity of the benzaldehyde functionalities was verified by cross-linking the polymersomes and also by a one-pot cross-linking and functionalization approach to further render the vesicles fluorescent, each *via* reductive amination. *In vitro* studies found these labeled nanostructures to undergo cell association.

KEYWORDS: amphiphilic block copolymers · vesicular nanostructures · reactive polymers

Polymer vesicles, also known as "polymersomes",[1−6] are supramolecular assemblies of amphiphilic block copolymers[7−14] or complementary random copolymers[15] with sizes ranging from tens of nanometers to several hundreds of microns ("giant vesicles"). Similar to liposomes, polymersomes are composed of closed bilayer membranes with hollow cavities and, therefore, have tremendous potential for encapsulation and controlled delivery.[16−20] Moreover, their structures can be manipulated on both polymeric and supramolecular levels to afford tunability of their properties, including size control over nanoscale to microscale dimensions,[21−24] external stimulus responses,[25−32] mechanical properties,[33−35] membrane permeability,[36−39] and *in vivo* fate.[40,41]

Starting from the middle of the 1990s, a variety of polymer vesicles have been developed and studied as efficient and promising candidates for the delivery of both hydrophilic (encapsulated inside the hollow cavity) and hydrophobic (loaded within the bilayer membrane wall) molecules. However, most of them consisted of amphiphilic block copolymers with limited functionalities for chemical transformations after vesicle construction. While polymersome surface functionalizations have been reported through reactions with the functionalities installed at the chain ends of the hydrophilic segments,[42,43] there are limited literature reports associated with modifications of wall domains of polymersomes. Up to date, only radical polymerization,[33,44] photoinduced [2 + 2] cycloaddition,[15,45−47] base-catalyzed self-condensation of siloxanes,[28,48] and ring opening of epoxides[49] have been employed to cross-link the walls of polymer vesicles.

With the increasing interests in potential biomedical applications that utilize the membrane of polymersomes as a functional unit,[18,41,50−53] introduction of highly reactive functionalities into polymer vesicles is being explored to expand the scope of chemistries that can be incorporated within such nanostructures. Herein, we report our approach for constructing size-tunable polymersomes with benzaldehyde functionalities (a diverse electrophile that undergoes reaction under mild conditions), as well as their cross-linking and fluorophore functionalization *via* reductive amination (Scheme 1).

RESULTS AND DISCUSSION

Synthesis of Amphiphilic Block Copolymer Precursor. Poly(ethylene oxide)-*b*-poly(4-vinyl benzaldehyde) (PEO_{45}-*b*-$PVBA_{26}$), the amphiphilic diblock copolymer precursor for benzaldehyde-functionalized polymersomes, was prepared following our previously established method of reversible addition−fragmentation chain transfer (RAFT) polymerization of VBA.[54] The synthesis was conducted by using a monomethoxy-terminated PEO-based macrochain transfer agent (macro-CTA, M_n = 2360 Da, Figure 1a) and azobisisobutyronitrile (AIBN) in dry DMF heated at 75 °C for 3 h ($[VBA]_0/[CTA]_0/[AIBN]_0$ = 55:1:0.25; 55%

*Address correspondence to klwooley@artsci.wustl.edu.

Received for review November 25, 2008 and accepted January 26, 2009.

Published online February 2, 2009.
10.1021/nn8007977 CCC: $40.75

© 2009 American Chemical Society

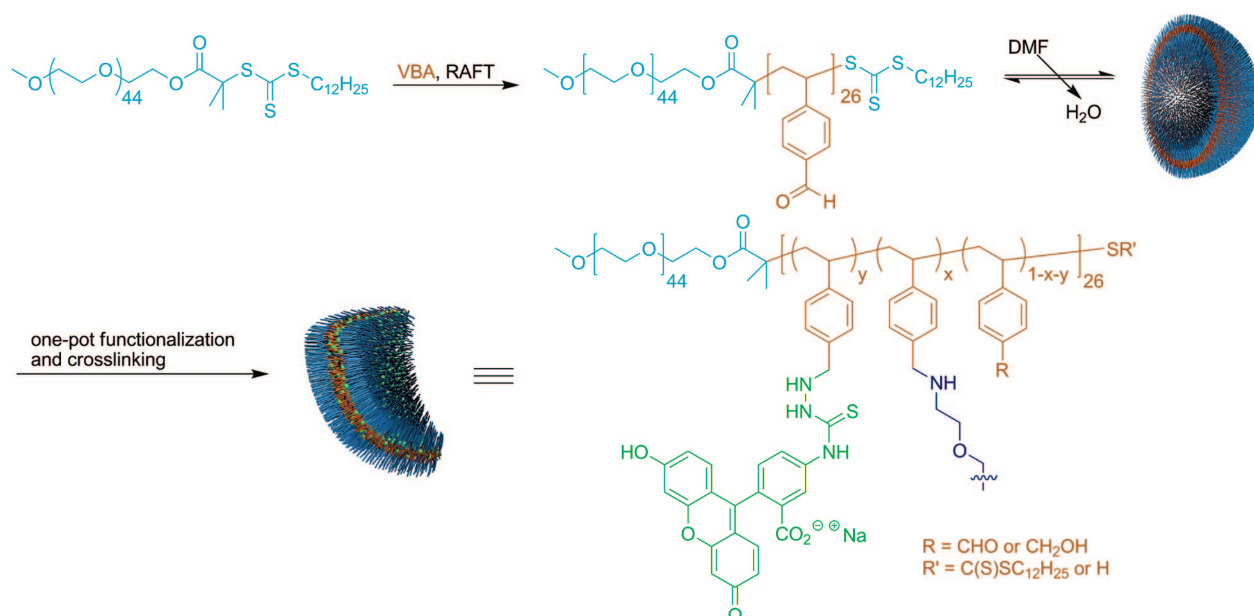

Scheme 1. Construction and functionalization of PEO_{45}-*b*-$PVBA_{26}$ vesicles through reductive amination.

conversion of VBA). ^{1}H NMR spectroscopic analysis of the isolated block copolymer (Figure 1b) confirmed successful chain extension for the formation of the PVBA block (resonances at 1.5 to 2.5, 4.8, 6.5 to 7.5, and 9.8 ppm) andmaintenance of the RAFT agent chain end group (resonances at 0.8 to 1.0, 1.3, and 3.2 ppm). The copolymer had a well-defined block structure of PEO_{45}-*b*-$PVBA_{26}$, which was supported by agreement between the number-average molecular weights by GPC (6200 Da) and by ^{1}H NMR spectroscopy (5800 Da, based upon comparison of the intensities of the resonances of the aldehyde proton of the VBA units at 9.8 ppm and methylene protons of EO units at 3.6 ppm with the characteristic resonances of the methine proton of the terminal monomer unit at 4.8 ppm and the SCH_2 protons from the RAFT functionality at 3.2 ppm). GPC analysis further showed that the block copolymer has a narrow and monomodal molecular weight distribution (Figure 1c) with a polydispersity index (PDI) of 1.2.

Construction and Characterization of PEO-*b*-PVBA Vesicles. General conditions under which amphiphilic block copolymers with a glassy hydrophobic segment (T_g = 86 °C for PVBA) can be assembled in aqueous solutions were then applied.[7,20,23,36,47] The PEO_{45}-*b*-$PVBA_{26}$ was first dissolved into *N*,*N*-dimethylformamide (DMF, a good solvent for both PEO and PVBA blocks, *ca.* 1 mg/mL), followed by addition of nanopure water (a selective solvent for the PEO block) until the water content reached 50 wt %. Finally, the DMF was removed by extensive dialysis against water.

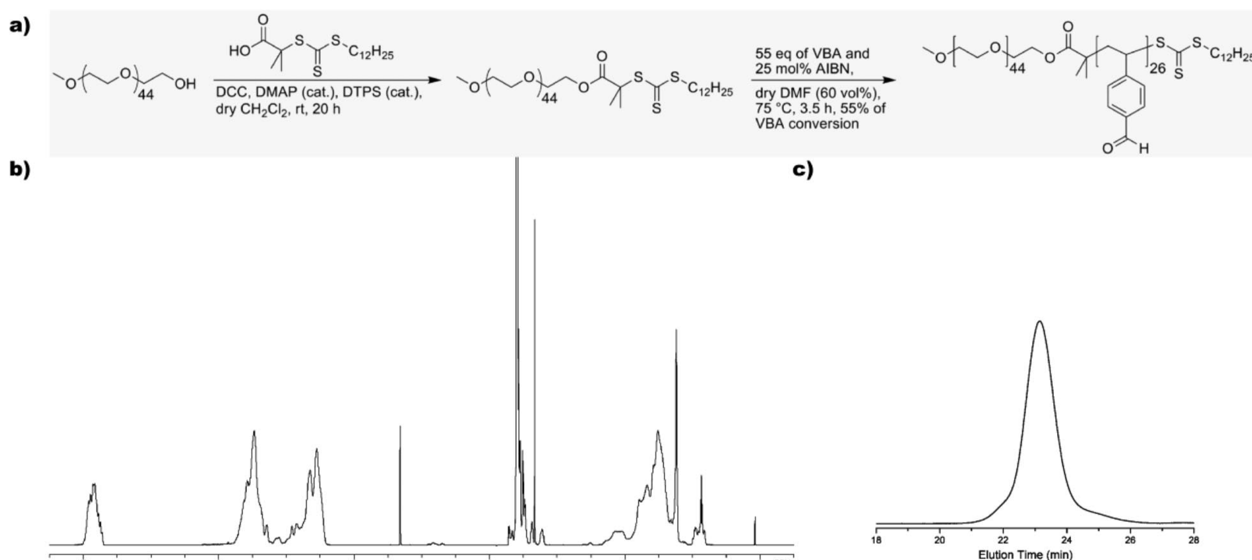

Figure 1. Synthesis and characterizations of PEO_{45}-*b*-$PVBA_{26}$ block copolymer precursor. (a) Schematic drawing of the synthesis of PEO_{45}-*b*-$PVBA_{26}$. (b) ^{1}H NMR spectrum of PEO_{45}-*b*-$PVBA_{26}$. (c) GPC profile of PEO_{45}-*b*-$PVBA_{26}$.

The vesicles were characterized by transmission electron microscopy (TEM, Figure 2a,b), scanning electron microscopy (SEM, Figure 2c,d), and dynamic light scattering (DLS, Figure 2e). The vesicular structure was confirmed by TEM and SEM. DLS analyses showed the hydrodynamic diameters of these vesicles were in the range of *ca*. 100 to 600 nm, with an intensity-average hydrodynamic diameter distribution centered at 290 nm and number-average hydrodynamic diameter distribution centered at 250 nm.

It is well-known that the formation of polymersomes usually passes through a morphological transformation of sphere−rod−vesicle.[4] To test whether this general trend also applied to our system, D_2O was added to a solution of PEO_{45}-*b*-$PVBA_{26}$ in DMF-d_7 (2.0 mg/mL) and aliquots were taken at predetermined water contents (9, 17, 23, and 33 wt %) for ^{1}H NMR and TEM measurements, and the results are summarized in Figure 3.

At a low water content of 9 wt %, the ^{1}H NMR spectrum (Figure 3a) showed no obvious difference with the spectrum of the block copolymer in neat DMF. However, the TEM image (Figure 3b) clearly indicated the formation of nanosized objects with multiple morphologies including spherical particles, semiclosed membranes, and vesicles, but no rods were observed. As the water content was increased to 17 wt %, the resonance signals corresponding to PEO backbone at 3.5 ppm became broader and the intensities of PVBA resonances (0.8−2.5, 6.7−7.6, and 9.9 ppm) decreased, indicating the reduced flexibility of both structural blocks. TEM imaging (Figure 3c) revealed the formation of small nanoparticles whose morphology could not be unambiguously distinguished and large aggregates (>200 nm, Figure 3c inset) that displayed large compound vesicular morphology. Finally, clear vesicular morphology appeared at 23 wt % of water content with varied size ranging from 100 to 600 nm (Figure 3d). At this point, essentially no proton resonances from PVBA blocks were observed in the ^{1}H NMR spectrum, presumably because they were "tightly" packed into the vesicle walls without significant mobility. Meanwhile, the resonances of PEO backbone protons were further broadened, likely due to the restricted mobility of the EO units, especially those in close proximity to the PVBA-based vesicle walls.

Interestingly, when the "intermediate" sample with a low water content of 9 wt % was directly dialyzed against water, smaller vesicles with number-average hydrodynamic diameter of *ca.* 90 nm were produced (Figure 4). These small vesicles were stable over 8 months, with no apparent growth in size. Although such size variation could not be interpreted quantitatively at this stage, these findings indicated kinetic control of self-assembled nanostructures of block copolymers and might provide new insight for adjusting vesicle size without changing the chemical composition of their polymer precursors.

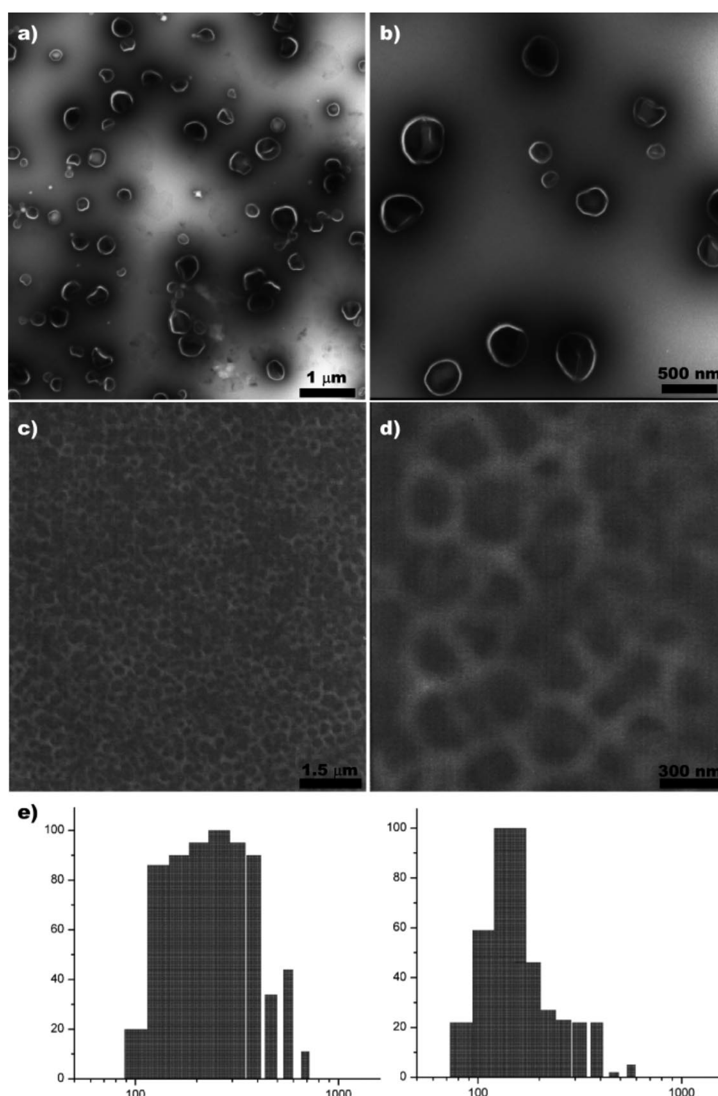

Figure 2. Characterization of polymer vesicles prepared from PEO_{45}-*b*-$PVBA_{26}$ block copolymer. (a,b) TEM images of vesicles (stained negatively with phosphotungstic acid). (c,d) SEM images of vesicles. (e) DLS histograms of vesicle size distributions (left: intensity-average hydrodynamic diameter; right: number-average hydrodynamic diameter).

Cross-Linking of PEO-*b*-PVBA Vesicles *via* Reductive Amination. The chemical accessibility of the aldehyde functionality in the vesicular wall was verified by reductive amination-based cross-linking with 2,2′-(ethylenedioxy)bis(ethylamine) (0.3 equiv relative to the aldehyde residues) and sodium cyanoborohydride (0.6 equiv relative to the aldehyde residues). No significant aggregation of vesicles was observed, based upon the DLS analysis (Figure 5a) and TEM imaging (Figure 5b), suggesting that only intravesicular cross-linking reactions occurred. It is noteworthy that, after cross-linking, the vesicles required buffer (5 mM pH 7.2 PBS with 5 mM of NaCl was used in our experiments) to remain suspended in aqueous solution. The zeta potential (ζ) measurement showed a dramatic decrease of sur-

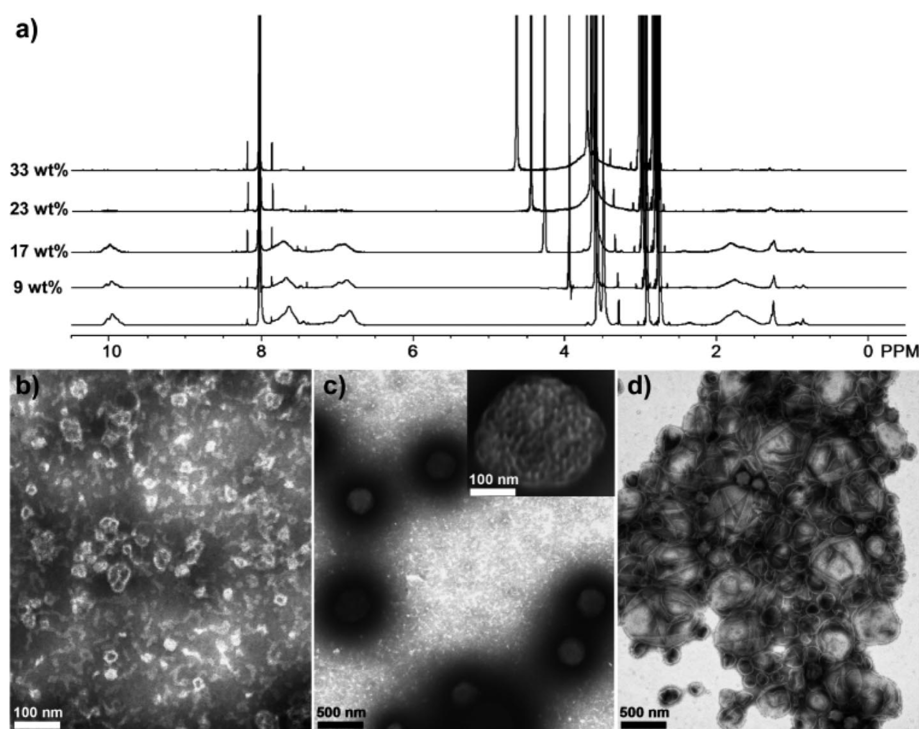

Figure 3. Morphological transformation during the self-assembly process of PEO_{45}-*b*-$PVBA_{26}$. (a) ^1H NMR spectra of aliquots in DMF-d_7 with different D_2O contents. (b−d) TEM micrographs of particles and vesicles (stained negative with phosphotungstic acid) at 9, 17, and 23 wt % of water content, respectively.

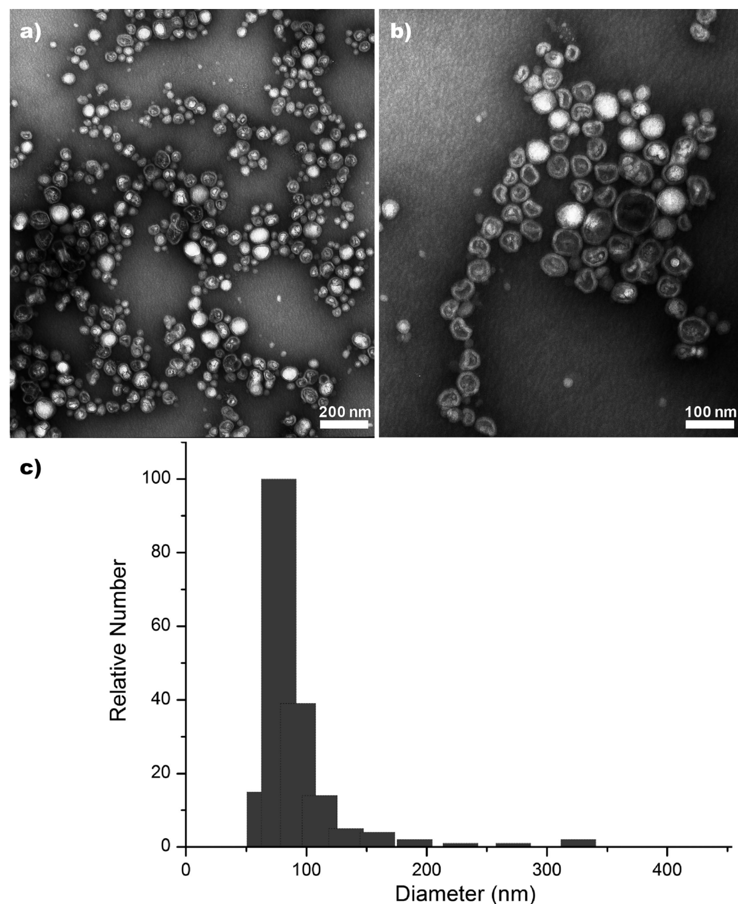

Figure 4. Characterization of small PEO_{45}-*b*-$PVBA_{26}$ vesicles. (a,b) TEM images of vesicles (stained negatively with PTA). (c) DLS histograms of vesicle size distributions (number-average hydrodynamic diameter).

face negative charge (−65.3 ± 0.7 mV *vs* −25.7 ± 0.8 mV), which might be associated with protonation of amines that were incorporated into the vesicles as a result of the reductive amination chemistry. The need for buffer and the less negative ζ potential value suggested that the structure of the vesicle was chemically changed after cross-linking, which was confirmed by ^1H NMR spectroscopy (Figure 5e). New resonances corresponding to the diamino cross-linker appeared at 3.3 ppm, and the ratio of aldehyde protons *versus* aromatic protons was decreased from 1.0:4.6 to 1.0:6.2, indicating *ca.* 26% of aldehyde residues were consumed during the reaction (*i.e.*, 43% incorporation efficiency based upon reaction stoichiometry, which was close to the results obtained by utilizing chromophores through the same chemistry, *vide infra*). Typically, cross-linking leads to shorter relaxation times and broadening and losses of solution-state NMR signal intensities. The observation of the new diamino cross-linker resonance may indicate covalent monoattachment within the vesicles, providing a relatively low degree of cross-linking. However, cross-linking indeed occurred, as was observed by the changes in the robust physical characteristics for the product vesicles. Of the 26% consumption of aldehydes, only a small fraction would be required to effectively cross-link an entire vesicle. Cross-linking significantly increased the vesicle stability, and no appreciable variations in size or size distribution were found after lyophilization and resuspension of these vesicles (Figure 5d).

***In Vitro* Cellular Studies.** Amine-derived dyes were then incorporated into the vesicles either sequentially or coincidentally with the cross-linking reaction *via* the same chemistry to demonstrate multiple couplings within a single nanostructure and to label the vesicles for biological studies. The vesicles were functionalized with fluorecein and cross-linked (0.02 equiv of dye, 0.5 equiv of cross-linker, 1 equiv of $NaCNBH_3$ relative to the aldehydes), each *via* reductive amination in a one-pot approach. UV−vis spectroscopy (Figure 6a) showed an absorption at 488 nm corresponding to the fluorescein, with an incorporation efficiency of *ca.* 35%. Again, no obvious size and morphological variations were observed for the fluorescein-functionalized non-cross-

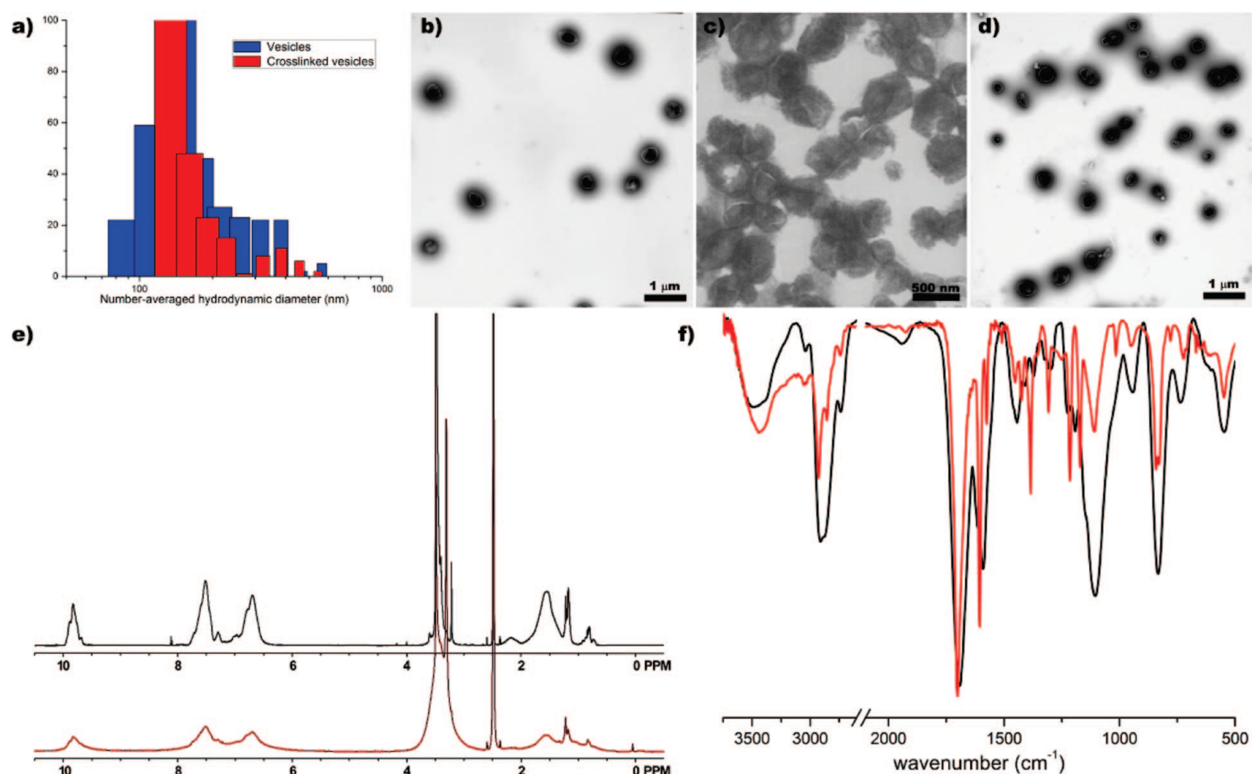

Figure 5. Characterization of cross-linked PEO_{45}-*b*-$PVBA_{26}$ vesicles through reductive amination. (a) DLS histograms of non-cross-linked (blue) and cross-linked (red) vesicle distributions. TEM (b) and SEM (c) images of cross-linked vesicles in 5 mM pH 7.2 PBS. (d) TEM image of lyophilized cross-linked vesicles after resuspension in 5 mM pH 7.2 PBS. (e) ^{1}H NMR spectra (DMSO-d_6) of lyophilized cross-linked vesicles (red) and polymer precursor (black). (f) IR spectra (KBr) of lyophilized cross-linked vesicles (red) and polymer precursor (black).

linked and cross-linked vesicles, as confirmed by TEM (Figure 6b).

In vitro CHO and HeLa cell experiments were then conducted for cross-linked and non-cross-linked fluorescein dye labeled vesicles. By fluorescence confocal microscopy, the vesicles were observed to undergo association with the cells in a time-dependent manner. No apparent fluorescence signal was detected after 1 and 4 h of incubation at 37 °C (data not shown). After 24 h, vesicles were visible under confocal microscopy (Figure 7e−h) and quantified by flow cytometry (Figure 7i) for both cell lines. Interestingly, an increased fraction of vesicles was observed to be associated with HeLa cells after the vesicles were cross-linked, while the opposite trend was noticed for CHO cells, with a

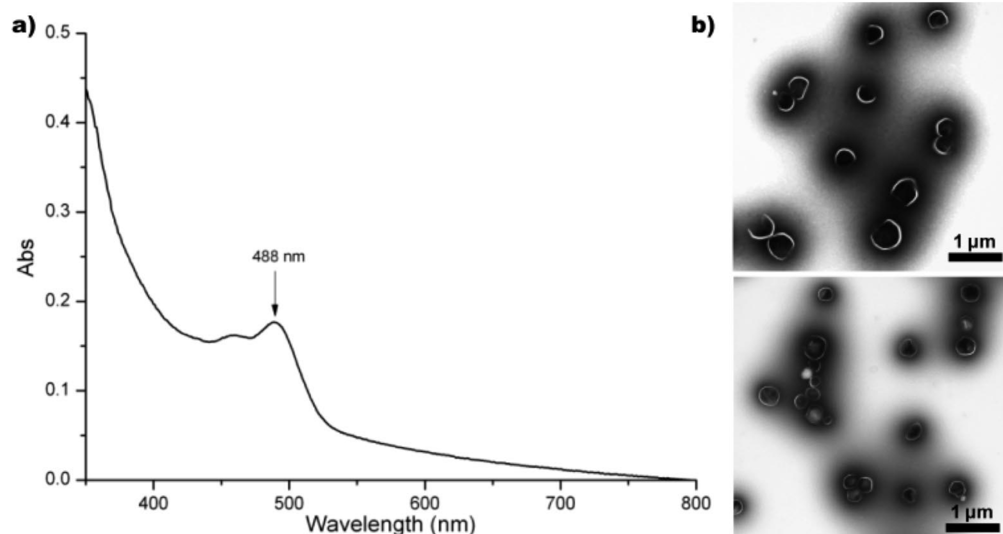

Figure 6. (a) UV−vis profile of fluorescein dye-functionalized cross-linked vesicles. (b) TEM images of non-cross-linked (top) and cross-linked (bottom) fluorescent vesicles.

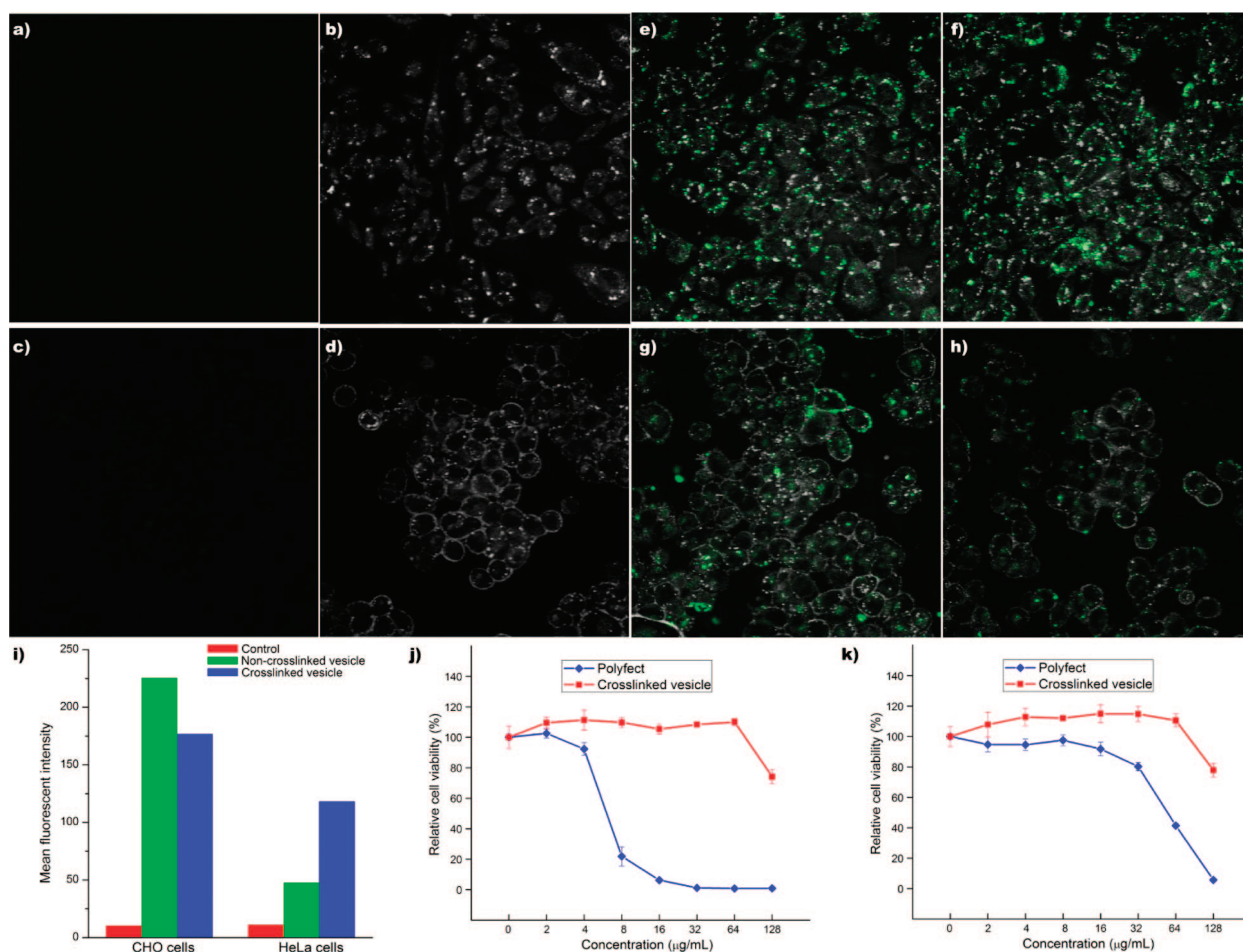

Figure 7. *In vitro* **evaluations of fluorescein-labeled vesicles. (a,b) Fluorescent confocal and bright-field images of CHO cells, respectively, without incubation with fluorescent vesicles. (c,d) Fluorescent confocal and bright-field images of HeLa cells, respectively, without incubation with fluorescent vesicles. (e,f) Overlay of bright-field and fluorescent confocal images of CHO cells incubated with cross-linked and non-cross-linked vesicles, respectively. (g,h) Overlay of bright-field and fluorescent confocal images of HeLa cells incubated with cross-linked and non-cross-linked vesicles, respectively. (i) Flow cytometry results. (j,k) Cytotoxicity results for CHO and HeLa cells, respectively.**

greater fraction of non-cross-linked vesicles undergoing strong cellular interactions. It is uncertain whether the vesicles are internalized within the cells. Although flow cytometry data confirmed that the vesicles remained associated with the cells under demanding conditions, the confocal microscopy images suggest that the vesicles are localized preferentially near the cell membrane. We hypothesize that such behavior may be the result of physical association or that it could be due to covalent coupling reactions between the aldehyde-loaded vesicles and amino groups on (membrane-bound) proteins. Although equimolar amounts of aldehyde and reducing agent were employed during the preparation of the fluoroescein-labeled, cross-linked vesicles, a portion of aldehydes still remains, as indicated by the ^{1}H NMR (Figure 5e) and IR data (Figure 5f) collected during the cross-linking experiments (*vide supra*).

The cytotoxicity of the cross-linked vesicles was also tested, using the cationic dendrimer polyfect as a positive control. Compared with polyfect, these vesicles had insignificant cytotoxicity for both cell lines (Figure 7j,k), indicating their biocompatibility and making them promising materials for fundamental studies in biotechnology.

CONCLUSIONS

In summary, we have synthesized polymer vesicles bearing benzaldehyde functionalities in the vesicular walls from self-assembly of the block copolymer PEO_{45}-*b*-$PVBA_{26}$. The aldehyde functionalities were shown to allow for modifications through facile and practical chemistry. Further investigations of the chemistry of these synthetic and reactive vesicles, including optimizing the reaction efficiency, exploring its scope, and incorporating other labels and ligands, are ongoing now. These robust nanostructures, with their ability to associate with the cell membrane, may find application as a nanoscopic device for repair or modification of cellular membrane functions.

EXPERIMENTAL SECTION

Materials. Monomethoxy-terminated monohydroxypoly(ethylene glycol) (mPEG2k, M_w = 2000 Da, PDI = 1.06) was purchased from Intezyne Technologies (Tampa, FL) and was used without further purification. (*S*)-1-Dodecyl-*S*′-(α,α′-dimethyl-α′′-acetic acid)trithiocarbonate (DDMAT),[55] 4-(dimethylamino)pyridinium 4-toluenesulfonate (DTPS),[56] and VBA[54] were synthesized according to literature reports. Other reagents and solvents were purchased from commercial sources (Sigma-Aldrich, Acrose, and Fluka) and were used without further purification unless otherwise noted. Methylene chloride (CH_2Cl_2) was distilled from calcium hydride and stored under N_2 before using.

Cell Culture. Chinese hamster ovary cells (CHO-K1) and human cervix carcinoma (HeLa) cells were cultivated in DMEM containing 10% FBS, streptomycin (100 μg/mL), and penicillin (100 units/mL) at 37 °C in a humidified atmosphere containing 5% CO_2.

Measurements. ^{1}H NMR spectra were recorded on a Varian 500 MHz spectrometer interfaced to a UNIX computer using Mercury software. Chemical shifts were referred to the solvent proton resonance. Infrared spectra were obtained on a Perkin-Elmer Spectrum BX FT-IR system using diffuse reflectance sampling accessories with FT-IR Spectrum v2.00 software.

Absolute molecular weight and molecular weight distribution were determined by gel permeation chromatography (GPC). GPC was performed on a Waters 1515 HPLC system (Water Chromatography Inc.), equipped with a Waters 2414 differential refractometer, a PD2020 dual-angle (15 and 90) light scattering detector (Precision Detectors Inc.), and a three-column series PL gel 5 μm mMixed columns (Polymer Laboratories Inc.). The eluent was anhydrous tetrahydrofuran (THF) with a flow rate of 1 mL/min. All instrumental calibrations were conducted using a series of nearly monodispersed polystyrene standards. Data were collected upon an injection of a 200 μL polymer solution in THF (*ca.* 5 mg/mL), and then analyzed using Discovery 32 software (Precision Detectors Inc.).

Samples for transmission electron microscopy (TEM) measurements were diluted with a 1% phosphotungstic acid (PTA) stain (v/v, 1:1). Carbon grids were exposed to oxygen plasma treatment to increase the surface hydrophilicity. Micrographs were collected at 10 000, 20 000, 50 000, and 100 000× magnification and calibrated using a 41 nm polyacrylamide bead from NIST.

Scanning electron microscopy (SEM) measurements were performed on a field emission scanning electron microscope (Hitachi s-4500), equipped with a NORAN Instruments energy dispersive X-ray (EDX) microanalysis system, a back scattering detector, and a mechanical straining stage. SEM samples were prepared with the following procedure. Silica native oxide wafers (Addison Engineering Inc.) were cleaned with nitric acid and hydrochloride acid (1:3) and then cut into 5 mm × 5 mm square. For each sample, 50 μL of aqueous solution was applied directly on the cleaned Si surface, and the solvent was kept in a fume hood to evaporate at ambient temperature (21 ± 2 °C). The samples were immediately transferred to the SEM instrument for measurement after completely dried.

Hydrodynamic diameters (D_h) and size distributions for the vesicles in aqueous solutions were determined by dynamic light scattering (DLS). The DLS instrumentation consisted of a Brookhaven Instruments Limited (Worcestershire, U.K.) system, including a model BI-200SM goniometer, a model BI-9000AT digital correlator, a model EMI-9865 photomultiplier, and a model 95-2 Ar ion laser (Lexel Corp.) operated at 514.5 nm. Measurements were made at 25 ± 1 °C. Scattered light was collected at a fixed angle of 90°. The digital correlator was operated with 522 ratio spaced channels, and initial delay of 5 μs, a final delay of 100 ms, and a duration of 6 min. A photomultiplier aperture of 100 μm was used, and the incident laser intensity was adjusted to obtain a photon counting between 200 and 300 kcps. Only measurements in which the measured and calculated baselines of the intensity autocorrelation function agreed to within 0.1% were used to calculate particle size. The calculations of the particle size distributions and distribution averages were performed with the ISDA software package (Brookhaven Instruments Company), which employed single-exponential fitting, cumulants analysis, and CONTIN particle size distribution analysis routines. All determinations were repeated five times.

Zeta potential values for the vesicle solution samples in 5 mM phosphate buffered saline (PBS) were determined with a Brookhaven Instrument Co. (Holtsville, NY) model Zeta Plus zeta potential analyzer. Data were acquired in the phase analysis light scattering (PALS) mode following solution equilibration at 25 °C. Calculation of ζ from the measured nanoparticle electrophoretic mobility (μ) employed the Smoluchowski equation: $\mu = \varepsilon\zeta/\eta$, where ε and η are the dielectric constant and the absolute viscosity of the medium, respectively. Measurements of ζ were reproducible to within ±2 mV of the mean value given by 16 determinations of 10 data accumulations.

The confocal microscopy was collected by using a Leica TCS SP2 confocal microscopy following excitation with an argon laser (488 nm); 5 × 10^5 cells were incubated on 35 mm MatTek glass bottom microwell dishes (MatTek Co.) for 24 h. Then the medium was replaced with 2 mL of fresh medium containing with non-cross-linked or cross-linked vesicles (10 μg/mL of polymer) and incubated for another 24 h. Cells were washed twice with PBS, and the live cells were imaged.

Flow cytometric analysis for the strong association of the vesicles to the cells was performed using a FACS-calibur (Becton Dickinson) equipped with an argon laser exciting at a wavelength of 488 nm. The cells were treated the same as above. For each sample, 20 000 events were collected by list-mode data that consisted of side scatter, forward scatter, and fluorescence emission centered at 530 nm. The fluorescence was collected at a logarithmic scale with a 1024 channel resolution. CellQuest software (Becton Dickinson) was applied for the analyses.

The cytotoxicity of cross-linked vesicles was examined by CellTiter-Glo Luminescent Cell Viability Assay (Promega Co.). The CHO-K1 cells and HeLa cells were seeded in the 96-well plate at a density of 1 × 10^4 cells/well and cultured for 24 h in 100 μL DMEM containing 10% FBS. Thereafter, the medium was replaced with 100 μL of fresh medium containing different concentration particles. After 24 h of incubation, 100 μL of the CellTiter-Glo reagent was added. The contents were mixed and the plate allowed to incubate at room temperature for 10 min to stabilize luminescent signal, and the luminescence at Luminoskan Ascent luminometer (Thermo Scientific) was recorded with an integration time of 1 s/well. The relative cell viability was calculated as cell viability (%) = (luminescence$_{(sample)}$/luminescence$_{(control)}$) × 100, where luminescence$_{(control)}$ was obtained in the absence of particles and luminescence$_{(sample)}$ was obtained in the presence of particles.

Synthesis of mPEG2k Macro-CTA. To a solution of mPEG2000 (4.0 g, 2.0 mmol) in 40 mL of dry CH_2Cl_2 at room temperature (rt) were added DDMAT (1.2 g, 3.0 mmol) and dicyclohexylcarbodiimide (0.60 g, 2.9 mmol), and the reaction mixture was stirred 10 min. After the additions of 4-di(methylamino)pyridine (36.6 mg, 0.3 mmol) and DPTS (375.0 mg, 1.2 mmol), the reaction mixture was further stirred 20 h at rt. Then the reaction mixture was filtered with Celite and the filtrate was placed at 4 °C overnight, filtered with Celite, and concentrated to *ca.* 15 mL. After the solution was precipitated into 250 mL of dry ether at 0 °C twice, the crude product obtained was further purified by flash column chromatography (2−3% MeOH/CH_2Cl_2, v/v) to afford mPEG2k macro-CTA as a yellow solid (3.2 g, 68% yield): ^{1}H NMR (500 MHz, CD_2Cl_2, δ) 0.88 (t, *J* = 6.5 Hz, 3H), 1.26 (m, 16H), 1.38 (t, *J* = 6.5 Hz, 2H), 1.66 (t, *J* = 7.5 Hz, 2H), 1.68 (s, 6H), 3.27 (t, *J* = 7.2 Hz, 2H), 3.33 (s, 3H), 3.40−3.80 (m, 166H), 4.21 (t, *J* = 5.0 Hz, 2H).

Synthesis of PEO_{45}-*b*-$PVBA_{26}$. To a 10 mL Schlenk flask equipped with a magnetic stir bar dried with flame under N_2 atmosphere were added the mPEG2k macro-CTA (0.48 g, 0.20 mmol) and dry DMF (2.5 mL). The reaction mixture was stirred 1 h at rt to obtain a homogeneous solution. To this solution were added VBA (1.46 g, 11.0 mmol) and AIBN (8.1 mg, 50 μmol). The reaction flask was sealed and stirred 10 min at rt. The reaction mixture was degassed through several cycles of freeze−pump−thaw. After the last cycle, the reaction mixture was stirred for 10 min at rt before immersing into a preheated oil bath at 75 °C to start the polymerization. After 3.5 h, the monomer conversion reached *ca.* 55% by analyzing aliquots collected through ^{1}H NMR spec-

troscopy. The polymerization was quenched by cooling the reaction flask with liquid N_2. CH_2Cl_2 (5.0 mL) was added to the reaction flask, and the polymer was purified by precipitation into 300 mL of cold diethyl ether at 0 °C twice. The precipitants were collected, washed with 100 mL of cold ether, and dried under vacuum overnight to afford the block copolymer precursor as a yellow solid (1.18 g, 90% yield based upon monomer conversion): ^1H NMR (500 MHz, CD_2Cl_2, δ) 0.88−1.24 (br, dodecyl Hs), 1.52−2.06 (br, PVBA backbone protons), 3.22 (br, SCH_2 of the chain terminus), 3.33 (s, mPEG terminal OCH_3), 3.34−3.78 (m, OCH_2CH_2O from the PEG backbone), 4.84 (br, 1H from the PVBA backbone benzylic terminus connected to trithiocarbonate), 6.58−6.85 (br, Ar H), 7.33−7.62 (br, Ar H), 9.88 (br, CHO); ^{13}C NMR (150 MHz, DMSO-d_6, δ) 192.3, 151.3, 134.4, 129.4, 128.0, 69.8, 42.3, 40.4, 29.0; IR (KBr) 3433, 2923, 2856, 2732, 1699, 1604, 1575, 1453, 1425, 1386, 1354, 1306, 1258, 1214, 1171, 1103, 1017, 951, 837, 726, 674, 552 cm^{-1}.

General Procedure for Construction of PEO_{45}-*b*-$PVBA_{26}$ Vesicles. To a solution of PEO_{45}-*b*-$PVBA_{26}$ block copolymer in DMF (*ca.* 1.0 mg/mL) was added dropwise an equal volume of nanopure H_2O *via* a syringe pump at a rate of 15.0 mL/h, and the mixture was further stirred for 16 h at rt. The solution was then transferred to presoaked dialysis tubing with molecular weight cut off (MWCO) of *ca.* 3500 Da and dialyzed against nanopure H_2O for 4 days to afford a solution of vesicles.

Cross-Linking of PEO_{45}-*b*-$PVBA_{26}$ Vesicles. To a solution of PEO_{45}-*b*-$PVBA_{26}$ vesicles (7.4 mg of polymer, 33 μmol of aldehyde residues) in 30.0 mL of nanopure H_2O was added a solution of 2,2′-(ethylenedioxy)bis(ethylamine) (1.5 mg, 10 μmol) in 1.0 mL of nanopure H_2O dropwise over 10 min. The reaction mixture was allowed to stir for 24 h at rt. $NaBH_3CN$ (1.3 mg, 20 μmol) in 1.3 mL of nanopure H_2O was then added to the reaction solution and further stirred for 16 h at rt. Finally, the mixture was transferred to presoaked dialysis tubing (MWCO = *ca.* 3500 Da) and dialyzed against 5.0 mM PBS (pH 7.2, with 5.0 mM NaCl) for 5 days to remove the small molecule byproduct and afford an aqueous solution of cross-linked vesicles.

One-Pot Functionalization and Cross-Linking of PEO_{45}-*b*-$PVBA_{26}$ Vesicles. To a solution of PEO_{45}-*b*-$PVBA_{26}$ vesicles (3.2 mg of polymer, 14 μmol of aldehyde residues) in 10.0 mL of nanopure H_2O was added a solution of fluorescein-5-thiosemicarbazide (126.3 μg, 0.30 μmol) in 90.0 μL of DMF. The reaction mixture was allowed to stir for 2 h at rt in the absence of light. To this reaction mixture was added a solution of 2,2′-(ethylenedioxy)bis(ethylamine) (1.1 mg, 7.2 μmol) in 1.6 mL of nanopure H_2O dropwise over 10 min. The reaction mixture was further stirred for 24 h at rt in the absence of light. $NaBH_3CN$ (907.2 μg, 14.4 μmol) in 0.4 mL of nanopure H_2O was then added to the reaction solution and further stirred for 16 h at rt in the absence of light. Finally, the mixture was transferred to presoaked dialysis tubing (MWCO = *ca.* 3500 Da) and dialyzed against 5.0 mM PBS (pH 7.2, with 5.0 mM NaCl) for 5 days to remove the small molecule byproduct and afford an aqueous solution of functionalized and cross-linked vesicles.

Acknowledgment. This material is based upon work supported by the National Heart Lung and Blood Institute of the National Institutes of Health as a Program of Excellence in Nanotechnology (U01 HL080729), and also by the National Science Foundation (DMR-0451490). The authors thank Mr. G.M. Veith for the kind assistance with TEM imaging, and Dr. J. Kao and Dr. A. d'Avignon for assistance with NMR measurements.

REFERENCES AND NOTES

1. Discher, D. E.; Eisenberg, A. Polymer Vesicles. *Science* **2002**, *297*, 967–973.
2. Antonietti, M.; Förster, S. Vesicles and Liposomes: A Self-Assembly Principle Beyond Lipids. *Adv. Mater.* **2003**, *15*, 1323–1333.
3. Opsteen, J. A.; Cornelissen, J. J. L. M.; van Hest, J. C. M. Block Copolymer Vesicles. *Pure Appl. Chem.* **2004**, *76*, 1309–1319.
4. Soo, P. L.; Eisenberg, A. Preparation of Block Copolymer Vesicles in Solution. *J. Polym. Sci. Part B: Polym. Phys.* **2004**, *42*, 923–938.
5. Kita-Tokarczyk, K.; Grumelard, J.; Haefele, T.; Meier, W. Block Copolymer Vesicles: Using Concepts from Polymer Chemistry to Mimic Biomembranes. *Polymer* **2005**, *46*, 3540–3563.
6. Discher, D. E.; Ahmed, F. Polymersomes. *Annu. Rev. Biomed. Eng.* **2006**, *8*, 323–341.
7. Zhang, L.; Eisenberg, A. Multiple Morphologies and Characteristics of "Crew-Cut" Micelle-like Aggregates of Polystyrene-*b*-Poly(acrylic acid) Diblock Copolymers in Aqueous Solutions. *J. Am. Chem. Soc.* **1996**, *118*, 3168–3181.
8. Discher, B. M.; Won, Y. Y.; Ege, D. S.; Lee, J. C. M.; Bates, F. S.; Discher, D. E.; Hammer, D. A. Polymersomes: Tough Vesicles Made from Diblock Copolymers. *Science* **1999**, *284*, 1143–1146.
9. Kukula, H.; Schlaad, H.; Antonietti, M.; Förster, S. The Formation of Polymer Vesicles or "Peptosomes" by Polybutadiene-block-Poly(L-glutamate)s in Dilute Aqueous Solution. *J. Am. Chem. Soc.* **2002**, *124*, 1658–1663.
10. Koide, A.; Kishimura, A.; Osada, K.; Jang, W. D.; Yamasaki, Y.; Kataoka, K. Semipermeable Polymer Vesicle (PICsome) Self-Assembled in Aqueous Medium from a Pair of Oppositely Charged Block Copolymers: Physiologically Stable Micro-/Nanocontainers of Water-Soluble Macromolecules. *J. Am. Chem. Soc.* **2006**, *128*, 5988–5989.
11. Li, Z.; Hillmyer, M. A.; Lodge, T. P. Laterally Nanostructured Vesicles, Polygonal Bilayer Sheets, and Segmented Wormlike Micelles. *Nano Lett.* **2006**, *6*, 1245–1249.
12. You, L.; Schlaad, H. An Easy Way to Sugar-Containing Polymer Vesicles or Glycosomes. *J. Am. Chem. Soc.* **2006**, *128*, 13336–13337.
13. Chiu, H.-C.; Lin, Y.-W.; Huang, Y.-F.; Chuang, C.-K.; Chern, C.-S. Polymer Vesicles Containing Small Vesicles within Interior Aqueous Compartments and pH-Responsive Transmembrane Channels. *Angew. Chem., Int. Ed.* **2008**, *47*, 1875–1878.
14. Pasparakis, G.; Alexander, C. Sweet Talking Double Hydrophilic Block Copolymer Vesicles. *Angew. Chem., Int. Ed.* **2008**, *47*, 4847–4850.
15. Thibault, R. J.; Uzun, O.; Hong, R.; Rotello, V. M. Recognition-Controlled Assembly of Nanoparticles Using Photochemically Crosslinked Recognition-Induced Polymersomes. *Adv. Mater.* **2006**, *18*, 2179–2183.
16. Ghoroghchian, P. P.; Frail, P. R.; Susumu, K.; Blessington, D.; Brannan, A. K.; Bates, F. S.; Chance, B.; Hammer, D. A.; Therien, M. J. Near-Infrared-Emissive Polymersomes: Self-Assembled Soft Matter for *In Vivo* Optical Imaging. *Proc. Natl. Acad. Sci. U.S.A.* **2005**, *102*, 2922–2927.
17. Ahmed, F.; Pakunlu, R. I.; Srinivas, G.; Brannan, A.; Bates, F.; Klein, M. L.; Minko, T.; Discher, D. E. Shrinkage of a Rapidly Growing Tumor by Drug-Loaded Polymersomes: pH-Triggered Release through Copolymer Degradation. *Mol. Pharm.* **2006**, *3*, 340–350.
18. Discher, D. E.; Ortiz, V.; Srinivas, G.; Klein, M. L.; Kim, Y.; Christian, D.; Cai, S.; Photos, P.; Ahmed, F. Emerging Applications of Polymersomes in Delivery: From Molecular Dynamics to Shrinkage of Tumors. *Prog. Polym. Sci.* **2007**, *32*, 838–857.
19. Adams, D. J.; Adams, S.; Atkins, D.; Butler, M. F.; Furzeland, S. Impact of Mechanism of Formation on Encapsulation in Block Copolymer Vesicles. *J. Controlled Release* **2008**, *128*, 165–170.
20. Krack, M.; Hohenberg, H.; Kornowski, A.; Lindner, P.; Weller, H.; Förster, S. Nanoparticle-Loaded Magnetophoretic Vesicles. *J. Am. Chem. Soc.* **2008**, *130*, 7315–7320.
21. Kabanov, A. V.; Bronich, T. K.; Kabanov, V. A.; Yu, K.; Eisenberg, A. Spontaneous Formation of Vesicles from Complexes of Block Ionomers and Surfactants. *J. Am. Chem. Soc.* **1998**, *120*, 9941–9942.
22. Bermudez, H.; Brannan, A. K.; Hammer, D. A.; Bates, F. S.; Discher, D. E. Molecular Weight Dependence of Polymersome Membrane Structure, Elasticity, and Stability. *Macromolecules* **2002**, *35*, 8203–8208.
23. Choucair, A.; Lavigueur, C.; Eisenberg, A. Polystyrene-*b*-Poly(acrylic acid) Vesicle Size Control Using Solution

Properties and Hydrophilic Block Length. *Langmuir* **2004**, *20*, 3894–3900.
24. Wang, X.; Winnik, M. A.; Manners, I. Synthesis and Self-Assembly of Poly(ferrocenyldimethylsilane-*b*-Dimethylaminoethyl methacrylate): Toward Water-Soluble Cylinders with an Organometallic Core. *Macromolecules* **2005**, *38*, 1928–1935.
25. Chécot, F.; Lecommandoux, S.; Gnanou, Y.; Klok, H.-A. Water-Soluble Stimuli-Responsive Vesicles from Peptide-Based Diblock Copolymers. *Angew. Chem., Int. Ed.* **2002**, *41*, 1339–1343.
26. Napoli, A.; Valentini, M.; Tirelli, N.; Müller, M.; Hubbell, J. A. Oxidation-Responsive Polymeric Vesicles. *Nat. Mater.* **2004**, *3*, 183–189.
27. Power-Billard, K. N.; Spontak, R. J.; Manners, I. Redox-Active Organometallic Vesicles: Aqueous Self-Assembly of a Diblock Copolymer with a Hydrophilic Polyferrocenylsilane Polyelectrolyte Block. *Angew. Chem., Int. Ed.* **2004**, *43*, 1260–1264.
28. Du, J.; Armes, S. P. pH-Responsive Vesicles Based on a Hydrolytically Self-Cross-Linkable Copolymer. *J. Am. Chem. Soc.* **2005**, *127*, 12800–12801.
29. Rodríguez-Hernández, J.; Lecommandoux, S. Reversible Inside-Out Micellization of pH-Responsive and Water-Soluble Vesicles Based on Polypeptide Diblock Copolymers. *J. Am. Chem. Soc.* **2005**, *127*, 2026–2027.
30. Li, Y.; Lokitz, B. S.; McCormick, C. L. Thermally Responsive Vesicles and Their Structural "Locking" through Polyelectrolyte Complex Formation. *Angew. Chem., Int. Ed.* **2006**, *45*, 5792–5795.
31. Qin, S.; Geng, Y.; Discher, D. E.; Yang, S. Temperature-Controlled Assembly and Release from Polymer Vesicles of Poly(ethylene oxide)-block-Poly(*N*-isopropylacrylamide). *Adv. Mater.* **2006**, *18*, 2905–2909.
32. Lomas, H.; Canton, I.; MacNeil, S.; Du, J.; Armes, S. P.; Ryan, A. J.; Lewis, A. L.; Battaglia, G. Biomimetic pH Sensitive Polymersomes for Efficient DNA Encapsulation and Delivery. *Adv. Mater.* **2007**, *19*, 4238–4243.
33. Discher, B. M.; Bermudez, H.; Hammer, D. A.; Discher, D. E.; Won, Y.-Y.; Bates, F. S. Cross-Linked Polymersome Membranes: Vesicles with Broadly Adjustable Properties. *J. Phys. Chem. B* **2002**, *106*, 2848–2854.
34. Kros, A.; Linhardt, J. G.; Bowman, H. K.; Tirrell, D. A. From Giant Vesicles to Filaments and Wires: Templates for Conducting Polymers. *Adv. Mater.* **2004**, *16*, 723–727.
35. Reiner, J. E.; Wells, J. M.; Kishore, R. B.; Pfefferkorn, C.; Helmerson, K. Stable and Robust Polymer Nanotubes Stretched from Polymersomes. *Proc. Natl. Acad. Sci. U.S.A.* **2006**, *103*, 1173–1177.
36. Wu, J.; Eisenberg, A. Proton Diffusion across Membranes of Vesicles of Poly(styrene-*b*-Acrylic acid) Diblock Copolymers. *J. Am. Chem. Soc.* **2006**, *128*, 2880–2884.
37. Kumar, M.; Grzelakowski, M.; Zilles, J.; Clark, M.; Meier, W. Highly Permeable Polymeric Membranes Based on the Incorporation of the Functional Water Channel Protein Aquaporin Z. *Proc. Natl. Acad. Sci. U.S.A.* **2007**, *104*, 20719–20724.
38. Leson, A.; Filiz, V.; Förster, S.; Mayer, C. Water Permeation through Block-Copolymer Vesicle Membranes. *Chem. Phys. Lett.* **2007**, *444*, 268–272.
39. Shum, H. C.; Kim, J.-W.; Weitz, D. A. Microfluidic Fabrication of Monodisperse Biocompatible and Biodegradable Polymersomes with Controlled Permeability. *J. Am. Chem. Soc.* **2008**, *130*, 9543–9549.
40. Photos, P. J.; Bacakova, L.; Discher, B.; Bates, F. S.; Discher, D. E. Polymer Vesicles in Vivo: Correlations with PEG Molecular Weight. *J. Controlled Release* **2003**, *90*, 323–334.
41. Broz, P.; Driamov, S.; Ziegler, J.; Ben-Haim, N.; Marsch, S.; Meier, W.; Hunziker, P. Toward Intelligent Nanosize Bioreactors: A pH-Switchable, Channel-Equipped, Functional Polymer Nanocontainer. *Nano Lett.* **2006**, *6*, 2349–2353.
42. Opsteen, J. A.; Brinkhuis, R. P.; Teeuwen, R. L. M.; Loewik, D. W. P. M.; van Hest, J. C. M. "Clickable" Polymersomes. *Chem. Commun.* **2007**, 3136–3138.
43. Hammer, D. A.; Robbins, G. P.; Haun, J. B.; Lin, J. J.; Qi, W.; Smith, L. A.; Ghoroghchian, P. P.; Therien, M. J.; Bates, F. S. Leuko-polymersomes. *Faraday Discuss.* **2008**, *139*, 129–141.
44. Hales, M.; Barner-Kowollik, C.; Davis, T. P.; Stenzel, M. H. Shell-Cross-Linked Vesicles Synthesized from Block Copolymers of Poly(D,L-lactide) and Poly(*N*-isopropyl acrylamide) as Thermoresponsive Nanocontainers. *Langmuir* **2004**, *20*, 10809–10817.
45. Ding, J.; Liu, G. Water-Soluble Hollow Nanospheres as Potential Drug Carriers. *J. Phys. Chem. B* **1998**, *102*, 6107–6113.
46. Zheng, R.; Liu, G. Water-Dispersible Oil-Filled ABC Triblock Copolymer Vesicles and Nanocapsules. *Macromolecules* **2007**, *40*, 5116–5121.
47. Walther, A.; Goldmann, A. S.; Yelamanchili, R. S.; Drechsler, M.; Schmalz, H.; Eisenberg, A.; Müller, A. H. E. Multiple Morphologies, Phase Transitions, and Cross-Linking of Crew-Cut Aggregates of Polybutadiene-block-Poly(2-vinylpyridine) Diblock Copolymers. *Macromolecules* **2008**, *41*, 3254–3260.
48. Du, J.; Chen, Y.; Zhang, Y.; Han, C. C.; Fischer, K.; Schmidt, M. Organic/Inorganic Hybrid Vesicles Based on A Reactive Block Copolymer. *J. Am. Chem. Soc.* **2003**, *125*, 14710–14711.
49. Zhu, H.; Liu, Q.; Chen, Y. Reactive Block Copolymer Vesicles with an Epoxy Wall. *Langmuir* **2007**, *23*, 790–794.
50. Choi, H. J.; Montemagno, C. D. Artificial Organelle: ATP Synthesis from Cellular Mimetic Polymersomes. *Nano Lett.* **2005**, *5*, 2538–2542.
51. Ranquin, A.; Versees, W.; Meier, W.; Steyaert, J.; Van Gelder, P. Therapeutic Nanoreactors: Combining Chemistry and Biology in a Novel Triblock Copolymer Drug Delivery System. *Nano Lett.* **2005**, *5*, 2220–2224.
52. Holowka, E. P.; Sun, V. Z.; Kamei, D. T.; Deming, T. J. Polyarginine Segments in Block Copolypeptides Drive Both Vesicular Assembly and Intracellular Delivery. *Nat. Mater.* **2007**, *6*, 52–57.
53. Ben-Haim, N.; Broz, P.; Marsch, S.; Meier, W.; Hunziker, P. Cell-Specific Integration of Artificial Organelles Based on Functionalized Polymer Vesicles. *Nano Lett.* **2008**, *8*, 1368–1373.
54. Sun, G.; Cheng, C.; Wooley, K. L. Reversible Addition Fragmentation Chain Transfer Polymerization of 4-Vinylbenzaldehyde. *Macromolecules* **2007**, *40*, 793–795.
55. Lai, J. T.; Filla, D.; Shea, R. Functional Polymers from Novel Carboxyl-Terminated Trithiocarbonates as Highly Efficient RAFT Agents. *Macromolecules* **2002**, *35*, 6754–6756.
56. Moore, J. S.; Stupp, S. I. Room Temperature Polyesterification. *Macromolecules* **1990**, *23*, 65–70.